CONTEMPORARY MATHEMATICS

Multiparameter Bifurcation Theory

Proceedings of a Summer Research Conference held July 14–20, 1985

AMERICAN MATHEMATICAL SOCIETY

VOLUME 56

CONTEMPORARY MATHEMATICS

Titles in This Series

Volume

Titles in This Series

Volume

Contemporary Mathematics
Volume 56, 1986

PHASE-TURBULENCE IN CONVECTION NEAR THRESHOLD

F.H. Busse

ABSTRACT. Phase-turbulence is the phenomenon of fluid motion characterized by a chaotic variation in space and in time, but associated with only a narrow band of modes in the wavenumber space. Convection in a layer heated from below exhibits phase turbulence in the limit of small amplitudes when the layer is rotating about a vertical axis or when the stress-free boundaries are used. These cases offer the simplest examples of fluid motion exhibiting turbulence in their spatial and time dependence.

1. INTRODUCTION. Rayleigh-Bénard convection in a fluid layer heated from below has become recognized in the past decade as one of the most suitable systems for the study of the evolution of turbulence. Much attention has been focussed on the low aspect ratio case in which the width of the convection box permits the realisation of only two or three convection rolls. For a survey of the phenomena observed in this case we refer to Gollub and Benson [1]. Phenomena similar to those occurring in a low aspect ratio convection box are found when a horizontal magnetic field is used to constrain the orientation of convection rolls [2]. The fact that only a few spatial convection modes can be excited in these experiments is responsible for the resemblance to solutions of systems of a few ordinary differential equations such as the Lorenz equations [3]. Various routes to chaotic behavior, such as the Ruelle-Takens [4] scenario and the period doubling sequence of Feigenbaum [5] have been observed both in the solutions of the differential equations and in convection experiments, although quantitative agreement cannot be expected. The detailed theoretical study of the transition to chaotic behavior in a low aspect ratio convection box is complicated by the fact that the transi-

tions of interest occur at Rayleigh numbers which are much higher than the threshold value at which convection sets in.

A different kind of turbulence occurs in horizontally extended convection layers. Ahlers and Behringer [6] found that the Rayleigh number for the onset of aperiodic time dependence decreases significantly with increasing aspect ratio of the convection box. The observations of Gollub and Steinman [7] have suggested that this aperiodic time dependence is connected with the onset of the skewed varicose instability. Numerical simulations by Zippelius and Siggia [8] of finite amplitude convection in the presence of stress-free boundaries indicate, that the attracting basin of stable steady convection rolls is so small and restricted that the convection flow seems to be unable to approach it after the destruction of the original unstable roll pattern by the skewed varicose instability.

A convection layer with stress-free boundaries offers special opportunities for the investigation of the skewed varicose instability. Because the latter occurs in the immediate neighborhood of the critical Rayleigh number, analytical expressions for the stability boundary can be derived [8,9,10]. In the latter paper it has been shown that convection rolls with the critical wavenumber α_c become unstable as soon as the Rayleigh number exceeds its critical value. Moreover a new instability, the oscillatory skewed varicose instability, has been found which becomes important at low Prandtl numbers P. It is responsible for the property that all convection rolls are unstable in the neighborhood of the critical Rayleigh number for $P \leq 0.543$. The absence of any stable steady solution raises the question as to the nature of the time dependence of the realized convection flow.

2. OUTLINE OF THE MATHEMATICAL ANALYSIS. Using the general representation for the velocity field $\mathbf{v}$,

$$\mathbf{v} = \nabla\times(\nabla\times\boldsymbol{\lambda}\phi)+\nabla\times\boldsymbol{\lambda}\psi \tag{1}$$

where $\boldsymbol{\lambda}$ is the vertical unit vector, we may write the general solution for small amplitude convection in the form [11]

$$\phi = f(z)\sum_{n=-N}^{N} C_n(t)\exp\{i\mathbf{k}_n\cdot\mathbf{r}\} + \dots \tag{2}$$

where z is the coordinate in the vertical direction and where the definitions

(3) $$\underset{\sim}{k}_{-n} = -\underset{\sim}{k}_n,\ \underset{\sim}{k}_n \cdot \underset{\sim}{\lambda} = 0,\ \sum_{n=-N}^{N} |C_n|^2 = \varepsilon(t)^2,\ C_{-n} = C_n^+$$

have been used. C_n^+ denotes the complex conjugate of C_n. The summation limit N in (2) could approach infinity. Terms of the order ε^2 have not been given explicitly in (2); but they will be taken into account in the analysis. The function f(z) is given by $\sin\pi(z+\frac{1}{2})$ in the case of stress-free boundaries at $z = \pm\frac{1}{2}$.

The time dependence of the coefficients $C_n(t)$ is determined by evolution equations of the form

(4.a) $$(1+P)\frac{d}{dt}C_p = (R-R_p)\gamma_p C_p - \sum_{n,m,r} \delta(\underset{\sim}{k}_n+\underset{\sim}{k}_m+\underset{\sim}{k}_r-\underset{\sim}{k}_p)[d_{nmrp}C_nC_m + s_{nmrp}G_{nm}]C_r$$

(4.b) $$\frac{d}{dt}G_{nm} = -|\underset{\sim}{k}_n+\underset{\sim}{k}_m|^2 G_{nm} + |\underset{\sim}{k}_n+\underset{\sim}{k}_m|^{-2}\ q_{nm}C_nC_m$$

where R is the Rayleigh number, P is the Prandtl number and where the definitions

$$R_p \equiv (\pi^2+|\underset{\sim}{k}_p|^2)^3|\underset{\sim}{k}_p|^{-2}\ ,\quad \gamma_p \equiv (\pi^2+|\underset{\sim}{k}_p|^2)/R_p$$

have been used. The δ-function is unity when its argument vanishes; otherwise it is zero. The more lengthy expressions for d_{nmrp}, s_{nmrp}, q_{nm} can be derived easily in analogy to the analysis of Busse ant Bolton [10]. The coefficients $G_{rp}(t)$ originate from the representation of the flow associated with vertical vorticity,

(5) $$\psi = \sum_{n,m} G_{nm}(t)\exp\{i(\underset{\sim}{k}_n+\underset{\sim}{k}_m)\cdot\underset{\sim}{r}\}\ .$$

Only the component of ψ which is independent of z must be included in equations (4). Since $|\underset{\sim}{k}_n+\underset{\sim}{k}_m|$ may be a small quantity in contrast to $|\underset{\sim}{k}_p|$ which is of the order unity, the time dependence of the coefficients G_{nm} may be of the same order or larger than the viscous friction term which is the first term on the right hand side of (4.b). Equations (4) include all terms that appear in the stability analysis [10] if all vectors $\underset{\sim}{k}_p$ are admitted for which R_p is close to critical value $R_c \equiv 27\ \pi^4/4$ of the Rayleigh number. To facilitate the computational solution of equations (4) it is advantageous to introduce periodic boundary conditions in the horizontal dimensions and consider the solution for the interval

(6) $$-a \leq x,y \leq a\ .$$

Among the vectors

(7) $\underset{\sim}{k}_p = (\frac{\ell\pi}{a}, \frac{m\pi}{a})$, $-\infty<\ell,m<\infty$

those vectors will be admitted for which R_p is sufficiently close to R_c, say $R_p \leq R_\ell$. The cutoff Rayleigh number R_ℓ may be chosen equal to R. But in the actual computations $R_\ell<R$ has usually been assumed in order to achieve a faster integration in time.

The results of numerical integrations of the system of equations (4) are in general accordance with the expectations based on the stability analysis of rolls [10]. As initial condition the solution for a steady roll with a wavenumer $|\underset{\sim}{k}_p|$ close to the critical value α_c was used. In addition small initial values were assumed for the other coefficients C_n, $n \neq \pm p$. Unless the aspect ratio 2a of the layer or $R-R_c$ are very small, it is found that the initial roll becomes unstable with respect to disturbances associated with the neighboring $\underset{\sim}{k}$-vectors. This instability resembles closely the monotonic skewed varicose instability. When the Prandtl number P is of order unity the final state is usually a steady roll solution with a wavenumber $|\underset{\sim}{k}_r|$ less than $|\underset{\sim}{k}_p|$. Sometimes, when a total of 40 or more $\underset{\sim}{k}$-vectors participate (including their negative counterparts) the final state is a limit cycle in which the energy shifts in a periodic fashion from a roll like solution to a rectangle type solution characterized by four $\underset{\sim}{k}$-vectors. When the Prandtl number is lowered this behavior is encountered frequently also for lower values of the aspect ratio 2a and lower numbers of equations. Even cases of two independent frequencies corresponding to a motion on a torus in the phase space have been found.

The most interesting behavior is the persistent aperiodic time dependence that occurs when the Prandtl number is equal or less than about 0.5 and when the number of $\underset{\sim}{k}$-vectors is about 40 or more. According to the analytical theory [10] all steady solutions are unstable in this case and simple attractors do no longer seem to exist. A typical example is shown in figure 1 and 2. The heat transport H and the kinetic energy T of the toroidal part of the motion are shown as a function of time,

(8.a) $$H \equiv \frac{1}{2}\sum_n |C_n|^2 (\pi^2+|\underset{\sim}{k}_n|^2)^2 |\underset{\sim}{k}_n|^2$$

(8.b) $$T \equiv \frac{1}{2}\sum_{n,m} |G_{nm}|^2 |\underset{\sim}{k}_n+\underset{\sim}{k}_m|^2$$

While the kinetic energy of the poloidal part of the motion described by ϕ follows closely the function H(t), the toroidal part

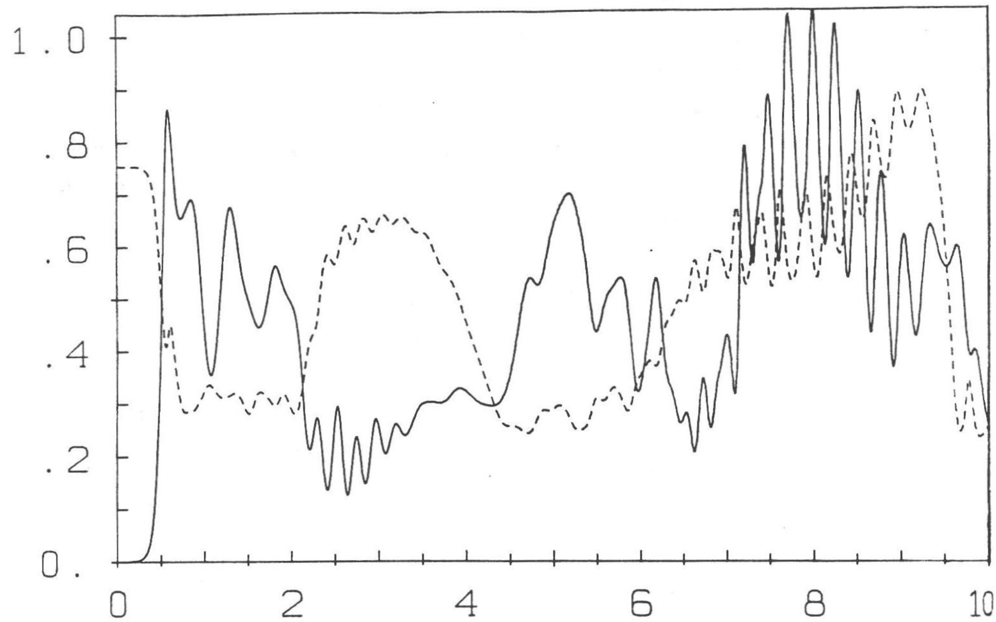

Figure 1: $10^{-4} \cdot H(t)$ (dashed) and $T(t)/200$ (solid) as function of time t (abscissa) in the case $R = 10^3$, $R_\ell = 800$, a = 4, P = 0.3. Initial condition is the steady solution for rolls for $C_2 = C_{-2}$ where $k_2 = (0.75\,\pi, 0)$. The other coefficients are set initially $C_n = 10^{-2}+i10^{-2}$.

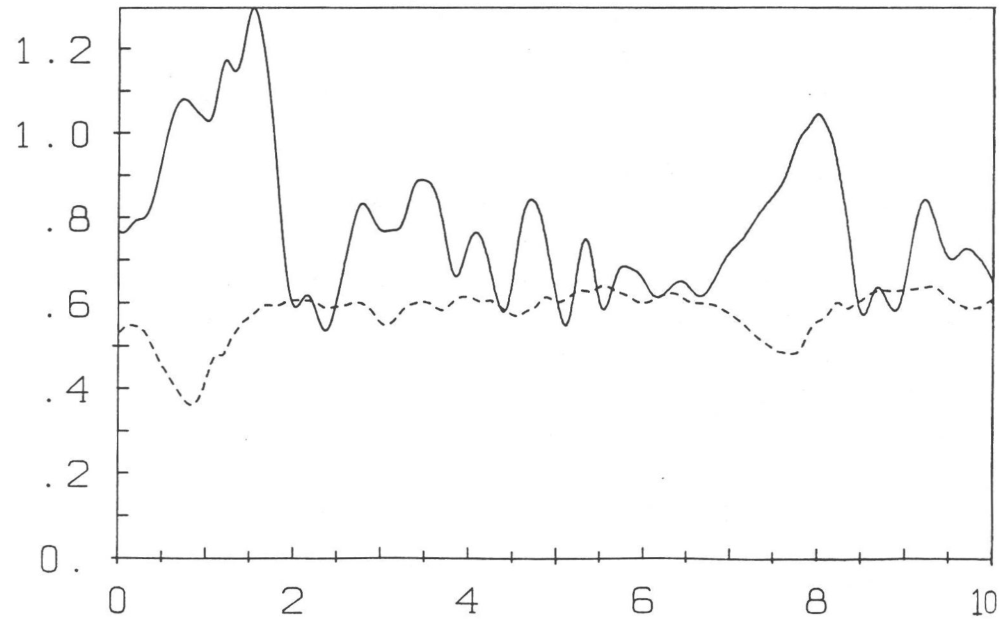

Figure 2: Same as Figure 1, but at a later time. The abscissa now gives t - 40.

T is often, but not always, anticorrelated with H. When instabilities of the monotonic or oscillatory skewed varicose type grow, energy is shifted into large scale horizontal motionsdescribed by ψ and a reduction of the heat transport occurs. In particular figure 1 shows the onset of the monotonic skewed varicose instability after the convection has started as a steady roll solution at $t = 0$. As low wavenumber rolls become dominant an oscillatory skewed varicose instability occurs at the time $t \simeq 6$. Later the system settles down, but aperiodic variations in time continue to occur as shown in figure 2. This apparently chaotic state is characterized by an average heat transport which is about 3/4 of the heat transport of steady periodic rolls with the critical wavenumber. The properties of the chaotic state require further study. A broad band of modes participate in the motion, although a roll like feature usually appears to dominate.

3. DISCUSSION . Convection in a non-rotating layer with stress-free boundaries in the second example of a fluid system in which persistent turbulence is encountered in the limit of vanishing amplitude of motion. The first example occurs in a rotating layer and can been described theoretically by the concept of the statistical limit cycle [12,13]. Both cases are characterized by the property that only a small band of the horizontal wave number participates while the direction of the wavevectors is nearly isotropically distributed and the phase of the motion is variable. Weak or phase turbulence thus seems to be an appropriate name for the phenomena encountered in these cases.

The more general relevance of phase turbulence derives from the fact that the near-degeneracy of the participating modes of convection which is its basic cause is typical for fully developed turbulent states. It is thus possible to study aspects of the general problem of turbulence in simple, but experimentally realisable cases which are at the same time accessible to detailed theoretical analysis. While convection with stress-free boundaries can not be realized as readily [14] as convection with rigid boundaries,the latter case appears to exhibit qualitatively similar phenomena albeit at higher amplitude of motion.

A variety of methods have been introduced in the theoretical analysis of the evolution of convection patterns. Since the primary goal of the earlier work has been the elucidation of the role of sidewalls in the formation of patterns, model equations rather than the basic equations have been used [15,16]. Even the numerical simulations by Manneville [17] which are similar to those of the present paper have not included all relevant non-linear terms. For a general introduction to the subject we refer to the recent book by Haken [18], who also considers the evolution of hexagonal cells in the presence of asymmetries in the layer. The periodic boundary conditions used in the present work are less realistic but permit a considerable reduction of computer costs. For the study of persistent turbulent states they appear to be especially appropriate.

REFERENCES

[1] Gollub, J.P., and S.V. Benson. Many routes to turbulent convection. J. Fluid Mech. 100, 449-470, 1980.

[2] Fauve, S., C. Laroche, and A. Libchaber. Effect of a horizontal magnetic field on convection instabilities in mercury. J. Physique Lett. 42, L 455-L457, 1981.
Libchaber, A., C. Laroche and S. Fauve. Period doubling cascade in mercury, a quantitative measurement. J. Physique Lett. 43, L211-L216, 1982.

[3] Lorenz, E.N., Deterministic Non-Periodic Flows. J. Atmos. Sci. 20, 130-141, 1963.

[4] Ruelle, D., and F. Takens. On the nature of turbulence. Comm. Math. Phys. 20, 167, 1971.

[5] Feigenbaum, M.J., Quantitative universality for a class of nonlinear transformations. J. Statist. Phys. 19, 25-52, 1978.

[6] Ahlers, G., and Behringer, R.P., Evolution of turbulence from the Rayleigh-Bénard instability. Phys. Rev. Lett. 40, 712-716, 1978.

[7] Gollub, J.P., and J.F. Steinman. Doppler Imaging of the Onset of Turbulent Convection. Phys. Rev. Lett. 47, 505-508, 1981.

[8] Zippelius, A., and E.D. Siggia. Stability of finite-amplitude convection. Phys. Fluids 26, 2905-2915, 1983.

[9] Zippelius, A., and Siggia, E.D., Disappearance of stable convection between free-slip boundaries. Phys. Rev. A 26, 1788-1790, 1982.

[10] Busse, F.H., and Bolton, E.W., Instabilities of convection rolls with stress-free boundaries near threshold. J. Fluid Mech. 146, 115-125, 1984.

[11] Busse, F.H., Nonlinear properties of thermal convection. Rep. Prog. Phys. 41, 1929-1967, 1978.

[12] Busse, F.H., and Heikes, K.E., Convection in a Rotating Layer: A simple Case of Turbulence, SCIENCE 208, 173-175, 1980.

[13] Busse, F.H., Transition to turbulence via the statistical limit cycle route, in "Turbulence and Chaotic Phenomena in Fluids" ed. by T. Tatsumi, Elsevier: 1984.

[14] Goldstein, R.J., and D.J. Graham. Stability of a horizontal fluid layer with zero shear boundaries. Phys. Fluids 12, 1133-1137, 1969.

[15] Greenside, H.S., W.M. Coughran, Jr., and N.L. Schryer. Nonlinear pattern formation near the onset of Rayleigh-Bénard convection. Phys. Rev. Lett. 49, 726-729, 1982.

[16] Manneville, P., A numerical simulation of "convection" in a cylindrical geometry. J. Physique 44, 563-571, 1983.

[17] Manneville, P., A two-dimensional model for three-dimensional convective patterns in wide containers. J. Physique 44, 759-765, 1983.
Manneville, P., Towards an understanding of weak turbulence close to the convection threshold in large aspect ratio systems. J. Physique Letts. 44, L903-L916, 1983.

[18] Haken H., Advanced Synergetics. Springer-Verlag 1983.

THEORETICAL PHYSICS
UNIVERSITY OF BAYREUTH
8580 Bayreuth
West-Germany

Contemporary Mathematics
Volume 56, 1986

NORMAL FORMS OF BIFURCATING PERIODIC ORBITS

Shui-Nee Chow* and Duo Wang**

ABSTRACT. We outline the normal form theory for periodic orbits and give the normal forms of codimension 2 bifurcation periodic orbits.

SECTION 1. Introduction. In this lecture, we will present a summary of the results in Chow and Wang [5].

Consider a differential equation with parameter $\lambda \in \mathbb{R}^k$

(1) $\dot{x} = f(x,\lambda)$, $x \in \mathbb{R}^k$,

where f is smooth. Suppose that $x = 0$ is a critical point for all values of the parameter. Let

$$D_x f(0,\lambda) = A(\lambda) .$$

If $A(\lambda)$ is hyperbolic, i.e., $A(\lambda)$ has no purely imaginary eigenvalues, then in a neighborhood of $x = 0$ the flow of (1) is topologically equivalent to the following linear flow

$$\dot{y} = A(\lambda)y .$$

Next, we assume that $A(\lambda_0)$ is non-hyperbolic, where λ_0 is fixed. For simplicity, we assume that $A(\lambda)$ is a versal deformation of $A(\lambda_0)$ (see Arnold [1] for more details on versal deformations). We say that the critical point $x = 0$ is a codimension k bifurcation point if $\lambda \in \mathbb{R}^k$ in the versal deformation $A(\lambda)$. For codimensions 1 and 2, it is not difficult to obtain the normal forms of (1) in a neighborhood of $x = 0$. In many cases, one could also give complete bifurcation diagrams for the flows of the normal forms near $x = 0$. We refer the reader to the following books: Arnold [1], Chow and Hale

---

1980 Mathematics Subject Classification. 34C20, 34C25.

*Partially supported by NSF grant DMS8401719 and DARPA

**Permanent address: Department of Mathematics, Jilin University, Changchun, People's Republic of China

[4] and Guckenheimer and Holmes [7] for more details. We also note that in the analysis of these vector fields, one encounters certain Abelian integrals which are related to Picard-Fuchs equations (see Carr, Chow and Hale [3], van Gils [9], for example).

Suppose we have a periodic orbit γ at λ_0. Let $B(\lambda_0)$ be its monodromy matrix. Suppose that $B(\lambda_0)$ is hyperbolic, i.e., $B(\lambda_0)$ has no eigenvalues on the unit circle, then the flow near the periodic orbit is topologically equivalent to the linear flow for some appropriate $(n-1) \times (n-1)$ matrix $C(\lambda_0)$

$$\dot{z} = C(\lambda_0)z , \qquad z \in \mathbb{R}^{n-1} ,$$
$$\dot{\theta} = 1 ,$$

where θ is an angle variable. Similarly, we may define the codimension of a non-hyperbolic periodic orbit. It is well-known that there are only three types of codimension 1 bifurcation for a periodic orbit. They are (a) saddle-node bifurcation; (b) period-doubling bifurcation and (c) Hopf bifurcation (invariant circles). Details may be found in Brunovsky [2], Chow and Hale [4] and Guckenheimer and Holmes [7].

For the case of a codimension 2 bifurcating periodic orbit, the bifurcation diagrams are not completely understood. In [8], Medved classify all codimension 2 monodromy matrices. By using his results, we are able to give all the normal forms of codimension 2 bifurcation periodic orbits. In many cases, we are also able to give the bifurcation diagrams of the flows near the periodic orbit. In section 2, we will outline the normal form theory for our purposes. In section 3, we apply the theory to codimensional 2 bifurcation periodic orbits.

We finally note that the theory of normal forms for periodic orbits of autonomous differential equations could be deduced from the theory of normal forms for diffeomorphisms. The converse is also true.

SECTION 2. Normal forms.

Suppose $x_0(t)$ is a T-periodic solution, $T > 0$, of (1) at $\lambda = 0$. Let $x = x_0(t) + y$. Then in a small neighborhood of $0 \in \mathbb{R}^n \times \mathbb{R}^k$, equation (1) becomes

$$\dot{y} = A(t)y + \sum_{|\alpha|=1}^{m} \lambda^\alpha f_\alpha(t) + \sum_{|\alpha|=1}^{m-1} \lambda^\alpha F_\alpha(t)y + \sum_{j=2}^{m} \sum_{|\alpha|=0}^{m-j} \lambda^\alpha \phi_\alpha^{(j)}(t,y) + O((|\lambda| + |y|)^{m+1}) \tag{2}$$

where $\alpha = (\alpha_1,\dots,\alpha_n)$ is a multi-index with nonnegative integers

α_i's, $|\alpha| = \alpha_1 + \cdots + \alpha_n$, $\lambda^\alpha = \lambda_1^{\alpha_1} \cdots \lambda_n^{\alpha_n}$; $f_\alpha(t) \in \mathbb{C}_T^n = \{f(t) \in \mathbb{C}^n \mid f(t+T) = f(t),\ t \in \mathbb{R}\}$, $A(t)$, $F_\alpha(t) \in \mathbb{C}_T^{n\times n} = \{H(t) \in \mathbb{C}^{n\times n} \mid H(t+T) = H(t),\ t \in \mathbb{R}\}$, $\Phi_\alpha^{(j)}(t,y) \in H_T^j = \{\Phi(t,y) \in \mathbb{C}^n \mid$ each component $\Phi_i(t,y)$ is homogeneous polynomial in $y \in \mathbb{R}^n$ with T-periodic coefficients in t, $1 \le i \le n\}$.

By Floquet Theory, there exists $P(t) \in \mathbb{C}_T^{n\times n}$ such that the linear T-periodic map

(3) $\quad y \to P(t)y,$

transforms (2) into

(4)
$$\dot{y} = Ay + \sum_{|\alpha|=1} \lambda^\alpha f_\alpha(t) + \sum_{|\alpha|=1}^{m-1} \lambda^\alpha F_\alpha(t)y + \sum_{j=2}^{m} \sum_{|\alpha|=0}^{m-j} \lambda^\alpha \Phi_\alpha^{(j)}(t,y) + O((|\lambda| + |y|)^{m+1})$$

where $A \in \mathbb{C}^{n\times n}$. Note that f_α, F_α and $\Phi^{(j)}(t,y)$ are different in (3) and (4).

Consider the following transformations:

$(T1)_i$ $\quad y = u + \sum_{|\beta|=i} \lambda^\beta h_\beta(t), \quad 1 \le i \le m, \quad h_\beta(t) \in \mathbb{C}_T^n;$

$(T2)_i$ $\quad y = u + \sum_{|\beta|=i} \lambda^\beta H_\beta(t)u, \quad 1 \le i \le m-1, \quad H_\beta(t) \in \mathbb{C}_T^{n\times n};$

$(T3)_{ij}$ $\quad y = u + \sum_{|\beta|=i} \lambda^\beta K_\beta^{(j)}(t,u), \quad 0 \le i,\ 2 \le j,\ i + j \le m,$

$K_\beta^{(j)}(t,u) \in H_T^j$

and the corresponding linear operators:

(i) $\quad O_1 : \mathbb{C}_T^n \to \mathbb{C}_T^n$

$O_1\, h(t) = h'(t) - Ah(t), \qquad h(t) \in \mathbb{C}_T^n;$

(ii) $\quad O_2 : \mathbb{C}_T^{n\times n} \to \mathbb{C}_T^{n\times n}$

$O_2\, H(t) = H'(t) - AH(t) + H(t)A, \qquad H(t) \in \mathbb{C}_T^{n\times n};$

(iii) $\quad O_{3j} : H_T^j \to H_T^j$

$O_{3j}\, K(t,u) = K'(t,u) + \frac{\partial}{\partial u} K(t,u)Au - AK(t,u),$

$K(t,u) \in H_T^j.$

Let $R_1 = \text{Range}(O_1)$, $R_2 = \text{Range}(O_2)$, $R_{3j} = \text{Range}(O_{3j})$, and G_1, G_2, G_{3j} be their supplementary subspaces in $\mathbb{C}^n_T$, $\mathbb{C}^{n\times n}_T$ and H^j_T respectively. Note that the G's are nonunique.

THEOREM 1. By using transformations $(T_1)_i$, $(T_2)_i$, $(T_3)_i$, equation (4) is transformed to the following:

$$\dot{u} = Au + \sum_{|\alpha|=1}^{m} \lambda^\alpha g_\alpha(t) + \sum_{|\alpha|=1}^{m-1} \lambda^\alpha G_\alpha(t)u \tag{5}$$

$$+ \sum_{j=2}^{m} \sum_{|\alpha|=0}^{m-j} \lambda^\alpha \Psi_\alpha^{(j)}(t,u) + O((|\lambda| + |u|)^{m+1}) ,$$

where $g_\alpha(t) \in G_1$, $G_\alpha(t) \in G_2$, $\Psi_\alpha^{(j)}(t,u) \in G_{3j}$, $2 \le j \le m$.

COROLLARY 2. Let $\sigma(A)$ be the spectrum of A. If $\mu \ne \ell\, 2\pi/T\, i$, $i = \sqrt{-1}$, for all $\mu \in \sigma(A)$ and $\ell \in Z$, then $G_1 = \{0\}$. If $\ell = 0$ is allowed, then G_1 consists only of constant vectors.

COROLLARY 3. If $\mu_j - \mu_k \ne \ell\, 2\pi/T\, i$, $\ell \ne 0$, $\ell \in Z$ holds for every μ_j, $\mu_k \in \sigma(A)$, then G_2 consists only of constant matrices.

REMARK 4. Under the assumptions of Corollary 3, Arnold's results on versal deformation of matrices [2] can be applied. In particular, if A is in (complex) Jordan form, then the structures of matrices in G_2 can be determined easily.

DEFINITION 5. Suppose $\mu_1,\dots,\mu_n$ are the eigenvalues of A and α is multi-index ($|\alpha| \ge 2$). If

$$(\alpha,\mu) - \mu_k = \ell \frac{2\pi}{T} i, \quad i = \sqrt{-1}, \quad \ell \in Z, \tag{6}$$

holds for some ℓ and μ_k, then the term $u^\alpha e_k$ is called a resonant term, where $e_k = (0,\dots,0,\underset{(k)}{1},0,\dots,0)^*$.

COROLLARY 6. If $A = \text{diag}(\mu_1,\dots,\mu_n)$ and for any $|\alpha| = j \ge 2$ and $\ell \in Z$, the resonant condition (6) does not hold, then $G_{3j} = \{0\}$; If (6) holds only for $\ell = 0$, then G_{3j} consists only of the resonant terms with constant coefficients.

REMARK 7. Assume G_1 consists only of constant vectors and G_2 consists only of constant matrices. Let $\dim G_1 = d_1$ and $\dim G_2 = d_2$. We can rewrite (5) as

$$\dot{u} = Au + \sum_{i=1}^{d_1} \Big(\sum_{|\alpha|=1}^{m} \lambda^\alpha C_{\alpha i}\Big)V_i + \sum_{i=1}^{d_2} \Big(\sum_{|\alpha|=1}^{m-1} \lambda^\alpha D_{\alpha i}\Big)W_i u \tag{7}$$

$$+ \sum_{j=2}^{m} \Big(\psi_0^{(j)}(t,u) + \sum_{|\alpha|=1}^{m-j} \lambda^\alpha \psi_\alpha^{(j)}(t,u)\Big) + O((|\lambda|+|u|)^{m+1}),$$

where $\{V_i\}$ is a basis of G_1, $\{W_i\}$ is basis of G_2, $C_{\alpha i}$ and $D_{\alpha i}$ are constants for each i.

DEFINITION 8. Let

$$\epsilon_i = \sum_{|\alpha|=1}^{m} \lambda^\alpha C_{\alpha i}, \qquad \mu_i = \sum_{|\alpha|=1}^{m-1} \lambda^\alpha D_{\alpha i} .$$

Then the truncated equation of (7):

$$\dot{u} = Au + \sum_{i=1}^{d_1} \epsilon_i V_i + \sum_{i=1}^{d_2} \mu_i W_i u + \sum_{j=2}^{m} \psi_0^{(j)}(t,u) . \tag{8}$$

is called a normal form of (1) up to order m associated with T-periodic solution $x_0(t)$.

We note that normal forms are not unique.

SECTION 3. Applications. First we assume that in (4)

$$f_\alpha(t) \equiv 0, \qquad 1 \leq |\alpha| \leq m.$$

We consider the following 8 cases of codimension 2 bifurcation of the periodic orbit $x_0(t)$ (see [8]). Let J be the monodromy matrix of linearized equation of (2). Without loss of generality, we assume $T = 1$.

Case (1).

$$J = \begin{bmatrix} 1 & 1 \\ 0 & 1 \end{bmatrix}, \quad \text{i.e.} \quad A = \begin{bmatrix} 0 & 1 \\ 0 & 0 \end{bmatrix} .$$

The normal form up to order 2 is

$$\begin{cases} u_1' = u_2 , \\ u_2' = \epsilon_1 u_1 + \epsilon_2 u_2 + \alpha u_1^2 + \beta u_1 u_2 . \end{cases} \tag{9}$$

Case 2.

$$J = \begin{bmatrix} -1 & 1 \\ 0 & -1 \end{bmatrix} .$$

We have

$$J^2 = \begin{bmatrix} 1 & 1 \\ 0 & 1 \end{bmatrix} \quad \text{and} \quad A = \begin{bmatrix} 0 & -1 \\ 0 & 0 \end{bmatrix}.$$

Since the 2-periodic matrix $P(t)$ of the Floquet transformation has the symmetric property:

$$P(t + T) = -P(t) ,$$

the normal form up to order 3 is

$$(10) \qquad \begin{cases} u_1' = u_2 , \\ u_2' = \epsilon_1 u_1 + \epsilon_2 u_2 + \alpha u_1^3 + \beta u_1^2 u_2 . \end{cases}$$

<u>Case (3)</u>.

$$J = \begin{bmatrix} \cos\omega & \sin\omega \\ -\sin\omega & \cos\omega \end{bmatrix}, \qquad 0 < \frac{\omega}{2\pi} = \frac{p}{q} < \frac{1}{2} ,$$

where p, q are integers with $(p,q) = 1$. We have

$$A = \begin{bmatrix} 0 & \omega \\ -\omega & 0 \end{bmatrix}.$$

Let $z = x_1 - ix_2$ and then let $z = ve^{\omega it}$. The complex form of the normal form is

$$(11) \qquad v' = \epsilon v + \alpha_1 |v|^2 v + \cdots + \alpha_k |v|^{2k} v + \beta \bar{v}^{q-1} ,$$

where $q - 3 < 2k + 1 \leq q - 1$.

Let $v = re^{i\theta}$. Then the real normal form is

$$(12) \qquad \begin{cases} r' = \epsilon_1 r + \alpha_{11} r^3 + \cdots + \alpha_{k1} r^{2k+1} + r^{q-1}(\beta_1 \cos q\theta + \beta_2 \sin q\theta) , \\ \theta' = \epsilon_2 + \alpha_{12} r^2 + \cdots + \alpha_{k2} r^{2k} + r^{q-2}(\beta_2 \sin q\theta - \beta_2 \cos q\theta) . \end{cases}$$

<u>Case (4)</u>.

$$J = \begin{bmatrix} \cos\omega & \sin\omega & 0 \\ -\sin\omega & \cos\omega & 0 \\ 0 & 0 & 1 \end{bmatrix}, \qquad 0 < \frac{\omega}{2\pi} < \frac{1}{2} ,$$

and $\omega/2\pi$ is not a root of unity. We have

$$A = \begin{bmatrix} 0 & \omega & 0 \\ -\omega & 0 & 0 \\ 0 & 0 & 0 \end{bmatrix}.$$

The normal form is

$$(12) \qquad \begin{cases} r' = \epsilon_1 r + \alpha_1 ry + \alpha_2 r^3 , \\ y' = \epsilon_2 y + \beta_1 y^2 + \beta_2 r^2 , \end{cases}$$

where the angle equation is omitted. The original equation can be regarded as a quasi-periodic (with 2 frequencies) perturbation of (12).